The 31st Asian Finance Association Annual Meeting 7 July 2019, Ho Chi MinH City, Vietnam

Reexamining the Pricing Kernel Puzzle: International Evidence

Gang Li*

January, 2019

Abstract

Recent studies use prices of aggregate market index options to infer the marginal utility of the representative investor, also known as the pricing kernel, and find that the marginal utility is not always monotonically decreasing, contradicting with the basic economic theory. The violation of the monotonicity is typically referred to as the pricing kernel puzzle. There are substantial disagreements on the existence and the nature of the pricing kernel puzzle in the literature. This paper proposes a unified approach to examining the existence of the pricing kernel puzzle and its economic importance from many aggregate market indexes around the world. We find that the violation of the monotonicity is a robust fact, existing across countries and sample periods. The likelihood of the violation in the high (low) return region increases (decreases) when the conditional volatility increases. The magnitude of the violation is economically significant and its variation is correlated across countries.

Keywords: projected pricing kernel; index option; nonparametric estimation

---

*Hong Kong Polytechnic University (HKPU), Email: garyli@polyu.edu.hk, Tel: (852) 2766-7136. I would like to thank Zhengyun Jiang for preparing the data. I acknowledges the financial support from the Research Grants Council of the Hong Kong SAR, China (grant no. PolyU 15526416). All remaining errors are mine.

1. Introduction

In the theoretical asset pricing, it is well known that the absence of arbitrage implies the existence of a pricing kernel or a stochastic discount factor which prices any asset. For pricing a specific asset or the derivative securities on it, the projected pricing kernel on the space of the asset return is sufficient. The projected pricing kernel on the aggregate wealth, which can be interpreted as the marginal utility of the representative investor in the financial market, is an important quantity in the financial economics. When the representative investor is risk averse, the projected pricing kernel on the aggregate wealth is expected to be monotonically decreasing. In the literature, the violation of the monotonicity is also referred to as the pricing kernel puzzle.

Many recent studies examine the monotonicity of the projected pricing kernel on the aggregate wealth and find mixed results. Some studies conclude that the violation of the monotonicity occurs around the current level of the wealth distribution, some suggest that it occurs at the upper tail of the wealth distribution, and others suggest no violation at all. The contradicting conclusions in these studies can be due to different assumptions, such as the pricing kernel being state-dependent or independent, the function form of the pricing kernel, the dynamics of the aggregate wealth, and state variables governing the dynamics. Many of the assumptions can be rather restrictive. Because of different findings in each study, different explanations are proposed to resolve the observed puzzle.

In this study, we propose unified approaches to estimating the projected pricing kernel and testing its monotonicity while overcoming issues in the existing studies. We allow the pricing kernel to be state-dependent without assuming the functional form of the pricing kernel, and conduct a nonparametric test to determine which state variables drive the variations of the projected pricing kernel in time series. We calculate the projected pricing kernel as the ratio of the conditional risk-neutral and conditional actual density functions of equity market index returns, both estimated nonparametrically, discounted at the risk-free rate. As thus, our estimation does not suffer from the problems arising from semiparametric/parametric approaches where restrictive parametric assumptions are imposed. We conduct a conditional test of the monotonicity of the projected pricing kernel at each day based on a bootstrap method, and examine on which days the monotonicity is likely to be violated. We also measure the magnitude of monotonicity violation by examining the slope of the projected pricing kernel and the region of the wealth distribution at which the violation occurs. The approach is applied to many major equity market indexes around world. This allows us to examine whether the phenomenon is systematic across countries, and also serves as robustness checks of the results.

Our results can be summarized as follows. First, the violation of monotonicity occurs in about one half of the time at the 5% significance level. The evidence is robust across major equity indexes around the world. Second, the nonmonotonicity can occur in low, medium or high regions in the return distribution, and the likelihood of nonmonotonicity in the high (low) return region increases (decreases) when the conditional volatility increases. Third, the nonmonotonicity is economically significant. This is evidenced by the fact that the nonmonotonicity appears at the high density region of the return distribution and the slope of the increasing section of the projected pricing kernel is steep. The measures of economic significance of the nonmonotonicity are positively correlated across the indexes in the time series. Overall, we find that the violation of monotonicity is a robust fact, which is not driven by random chances or data errors. Understanding the economic reasons behind the pattern of the nonmonotonicity deserves further studies.

The remaining of the paper is organized as follows. In Section 2, we review the relevant literature and point out issuing in estimating the projected pricing kernel. Section 3 introduces our estimation and testing methodology. In Section 4, we discuss our data and the empirical results. Second 5 concludes the paper.

2. Literature Review

The literature on the pricing kernel puzzle is large.[1] We focus on the estimation methodological issues that are particularly relevant to this study. The maintained assumptions of the projected pricing kernel in the literature can be classified as state-independent or state-dependent. The state independence refers to that the projected pricing kernel is a time-invariant function of the market return, whereas the state dependence refers to that the parameters of the projected pricing kernel depend on time and other state variables.[2] If the actual projected pricing kernel is state-dependent, inferences based on the state-independent projected pricing kernel, i.e., the projected pricing kernel estimated unconditionally, are unreliable. This is so because that the unconditionally projected pricing kernel is monotonically decreasing is neither sufficient nor necessary for the actual state-dependent projected pricing kernel to be monotonically decreasing.

The projected pricing kernel can be either estimated as the ratio of the risk-neutral probability density function to the actual probability density function of the market return, discounted at the risk-free rate, or explicitly specified as a parametric function of the market index return. The existing approaches can be generally classified as semiparametric/parametric or nonparametric in terms of the estimation methods.[3] For the semiparametric/parametric approaches, assumptions on dynamics of the underlying asset returns under the actual and/or the risk-neutral probability, or the functional form of the projected pricing kernel is assumed. Semiparametric/parametric approaches achieve better estimation efficiency when the assumptions are correct, however, they may suffer from the problems of model mis-specifications. The estimation results can be critically dependent

[1] A recent comprehensive review in this literature can be found in Cuesdeanu and Jackwerth (2018).

[2] Aït-Sahalia and Lo (2000), Bliss and Panigirtzoglou (2004), Linn, Shive and Shumway (2018), among others, restrict the projected pricing kernel to be state independent, whereas Jackwerth (2000), Rosenberg and Engle (2002), Barone-Adesi, Engle and Mancini (2008), among others, allow the state-dependent projected pricing kernel.

[3] For example, Aït-Sahalia and Lo (2000), Jackwerth (2000), and Beare and Schmidt (2016) use the nonparametric approaches, and Rosenberg and Engle (2002), Bliss and Panigirtzoglou (2004) and Barone-Adesi, Engle and Mancini (2008), among others, are considered as the semiparametric/parametric approaches.

on assumptions. For studies on the S&P 500 index options, based on different parametric assumptions, Rosenberg and Engle (2002) find the violation of the monotonicity, but Bliss and Panigirtzoglou (2004) and Barone-Adesi, Engle and Mancini (2008) do not find the violation. For nonparametric approaches, the actual and the risk-neutral density functions are estimated nonparametrically. This avoids the potentially restrictive assumptions imposed in the semiparametric/parametric approaches. However, for estimating the conditional actual density, conditional variables need to be explicitly specified and justified. Jackwerth (2000) uses a rolling window of past returns to estimate the conditional actual density. Beare and Schmidt (2016) consider the volatility as the only state variable and assume that the high-order moments of the conditional actual density are not relevant. They propose a conditional test on the shape of the estimated projected pricing kernel based on the ordinal dominance curve, and find that the monotonicity is rejected about 40% of the time at the 5% significance level. Song and Xiu (2016) use a short and a long term volatility as the state variables, and find the nonmonotonicity occurs at the upper tail of the index density. However, it is not clear that volatility is the only state variable governing the asset price dynamics.

Many studies examine the implication of the shape of the projected pricing kernel on the unconditional expected returns of options. Coval and Shumway (2001) find that both S&P 500 call and put average returns are increasing with strike prices empirically, which is consistent with the monotonically decreasing projected pricing kernel. Bakshi, Madan and Panayotov (2010) and Chaudhuri and Schroder (2015) find that average returns on S&P 500 index options decrease with strike prices, inconsistent with the monotonicity. The results reported in these studies are rather weak, and sensitive to sample periods and selections of strike prices and maturities of options. When the projected pricing kernel is state dependent, the implication of the monotonicity is actually on the conditional expected returns. This suggests that the null hypothesis can be rejected as long as one conditional test is rejected. Therefore, the tests on the unconditional expected returns as in these studies are lack of power and ignore the information on the variation of the projected pricing kernel across time. In addition, in Coval and Shumway (2001) and Bakshi, Madan and Panayotov (2010), the monotonicity (nonmonotonicity) is a sufficient but not necessary condition for increasing (decreasing) expected option returns across strike prices, so their findings are inconclusive on the shape of the projected pricing kernel.

Most of the studies on the projected pricing kernel examine the U.S. market, and a few studies examine the issue using international data, for example, Grith, Härdle, and Park (2013) for the DAX index in Germany, Liu et al. (2009) for the FTSE index in the U.K., and Perignon and Villa (2002) for the CAC 40 index in France, among others. These papers use different estimation methodology and find the nonmonotonicity to various degrees. Because of different methodologies, the results are not comparable across indexes. Overall, the evidence of the nonmonotonicity is still ambiguous in the existing literature.

3. Estimation and Testing

In this paper, we propose new approaches to estimating the projected pricing kernel, and testing its monotonicity while overcoming issues in the existing studies. We estimate the projected pricing kernel based on a conditional variables approach. Let $\tilde{p}(r_{t,\tau}|v_t)$ and $p(r_{t,\tau}|v_t)$ be the conditional risk-neutral density and the conditional actual density, respectively, of the gross return of market index from t to $t+\tau$, $r_{t,\tau}$, conditional on the state variable, v_t. $\tilde{p}(r_{t,\tau}|v_t)$ is estimated nonparametrically from the cross section of option prices with various strike prices, K, and maturity $t+\tau$, observed at t, and $p(r_{t,\tau}|v_t)$ is estimated from the time-series index returns based on the kernel method conditional on the pre-determined state variable, v_t. The projected pricing kernel at t is calculated as $\tilde{M}_{t,\tau}(r_{t,\tau}, v_t) = \frac{\tilde{p}(r_{t,\tau}|v_t)}{r_t^f p(r_{t,\tau}|v_t)}$, where r_t^f is the gross risk-free rate from t to $t+\tau$. The approach explicitly considers the conditional variable v_t when estimating $\tilde{M}_{t,\tau}(r_{t,\tau}, v_t)$, and improve upon the early approaches of using the rolling window of past returns to estimate $p(r_{t,\tau}|v_t)$. The approach also does not require parametric assumptions on the state-dependent pricing kernel, $p(r_{t,\tau}|v_t)$ or $\tilde{p}(r_{t,\tau}|v_t)$ as imposed in the existing literature.

3.1. *Identification of state variables*

In the conditional variables approach, we need to identify state variables which determine the dynamics of the pricing kernel. Since option prices observed at t are driven by the state variable, v_t, which is implicity incorporated in the conditional risk-neutral density, $\tilde{p}(r_{t,\tau}|v_t)$ in our approach. Thus, the choice of v_t, affects the estimation of the projected pricing kernel, $\tilde{M}_{t,\tau}(r_{t,\tau}, v_t)$, through that of the conditional actual density, $p(r_{t,\tau}|v_t)$. Therefore, we choose v_t by testing if v_t determines $p(r_{t,\tau}|v_t)$. Specifically, denote $v_t = (v_{0,t}, v_{1,t})$, where $v_{0,t}$ is the existing state variable used to estimate $p(r_{t,\tau}|v_{0,t})$, and $v_{1,t}$ is the new state variable to be tested. We test the independence between $r_{t,\tau}$ and $v_{1,t}$ conditional on $v_{0,t}$ against the conditional dependence, i.e., $\Pr\{p(r_{t,\tau}|v_t) = p(r_{t,\tau}|v_{0,t})\} = 1$ for any $r_{t,\tau}$ against $\Pr\{p(r_{t,\tau}|v_t) = p(r_{t,\tau}|v_{0,t})\} < 1$ for some $r_{t,\tau}$. We select $v_{1,t}$ as the additional state variable to estimate $p(r_{t,\tau}|v_t)$ if the null is rejected. When considering the first state variable, we test the unconditional dependence between $r_{t,\tau}$ and $v_{1,t}$, and $v_{0,t}$ belongs to the empty set.

We employ a nonparametric Hellinger distance based test of independence, supplemented by a bootstrap procedure, proposed by Su and White (2008) and Fernandes and Néri (2010). Such tests have been shown to have good size property and is powerful enough to detect various dependence structures. The statistic for testing the unconditional independence is based on

$$
\begin{aligned}
\Gamma &= \int\int \left[1 - \sqrt{\frac{p(r_{t,\tau})}{p(r_{t,\tau}|v_{1,t})}}\right]^2 w(r_{t,\tau}, v_{1,t}) p(r_{t,\tau}, v_{1,t}) dr_{t,\tau} dv_{1,t} \\
&= \int\int \left[1 - \sqrt{\frac{p(r_{t,\tau})p(v_{1,t})}{p(r_{t,\tau}, v_{1,t})}}\right]^2 w(r_{t,\tau}, v_{1,t}) p(r_{t,\tau}, v_{1,t}) dr_{t,\tau} dv_{1,t}, \qquad (1)
\end{aligned}
$$

where $w(r_{t,\tau}, v_{1,t})$ is a weighting function.[4] $w(r_{t,\tau}, v_{1,t})$ can be used to truncate the integration at the extremes, where the precise estimation of densities is difficult.[5] It is clear that

[4]From (1),

$$\Gamma = \int\int \left[\sqrt{p(r_{t,\tau}, v_{1,t})} - \sqrt{p(r_{t,\tau})p(v_{1,t})}\right]^2 w(r_{t,\tau}, v_{1,t}) dr_{t,\tau} dv_{1,t},$$

which is two times the weighted squared Hellinger distance between $p(r_{t,\tau}, v_{1,t})$ and $p(r_{t,\tau})p(v_{1,t})$.

[5]In practise, we simply set $w(r_{t,\tau}, v_{1,t}) = 1$ since the results are not sensitive to the choice of $w(r_{t,\tau}, v_{1,t})$.

$\Gamma \geq 0$, and the equality holds if and only if the null hypothesis is true. Thus, Γ serves as a proper statistic for consistently testing the null. The statistic for testing the independence conditional on $v_{0,t}$ is defined similarly as

$$\begin{aligned}\Gamma &= \int\int \left[1 - \sqrt{\frac{p(r_{t,\tau}|v_{0,t})}{p(r_{t,\tau}|v_t)}}\right]^2 w(r_{t,\tau}, v_t)p(r_{t,\tau}, v_t)dr_{t,\tau}dv_t \\ &= \int\int \left[1 - \sqrt{\frac{p(r_{t,\tau}, v_{0,t})p(v_t)}{p(r_{t,\tau}, v_t)p(v_{0,t})}}\right]^2 w(r_{t,\tau}, v_t)p(r_{t,\tau}, v_t)dr_{t,\tau}dv_t. \qquad (2)\end{aligned}$$

The sample analogs of Γ for the unconditional and conditional independence test statistics are given as,

$$\hat{\Gamma} = \frac{1}{T}\sum_{t=1}^{T}\left[1 - \sqrt{\frac{\hat{p}(r_{t,\tau})\hat{p}(v_{1,t})}{\hat{p}(r_{t,\tau}, v_{1,t})}}\right]^2 w(r_{t,\tau}, v_{1,t}), \qquad (3)$$

and

$$\hat{\Gamma} = \frac{1}{T}\sum_{t=1}^{T}\left[1 - \sqrt{\frac{\hat{p}(r_{t,\tau}, v_{0,t})\hat{p}(v_t)}{\hat{p}(r_{t,\tau}, v_t)\hat{p}(v_{0,t})}}\right]^2 w(r_{t,\tau}, v_t), \qquad (4)$$

respectively, where $\hat{p}(\cdot)$s and $\hat{p}(\cdot,\cdot)$s are density functions estimated nonparametrically, and T is the number of time-series observations. $\hat{\Gamma}$ standardized by a consistent estimator of its standard error, follows the standard normal distribution asymptotically under the null.

We use the standard Nadaraya-Watson estimator to estimate the density of an N-dimensional variable u, $p(u)$,

$$\hat{p}(u) = \frac{1}{T}\sum_{t=1}^{T}\prod_{j=1}^{J}\frac{1}{h_{j,t}}G\left(\frac{u_j - u_{j,t}}{h_{j,t}}\right), \qquad (5)$$

where $G(\cdot)$ is the kernel, $h_{j,t}$ is the bandwidth for $u_{j,t}$, and T is the number of observations.[6] We choose the second order Gaussian kernel $G(z) = (1/\sqrt{2\pi})e^{-z^2/2}$, which is commonly used in the literature.

We use a bootstrap procedure to improve the finite sample performance of the tests. We draw the bootstrap samples $\{r^*_{t,\tau}, v^*_{0,t}, v^*_{1,t}\}_{t=1}^{T}$ under the null as follows. For the uncon-

[6] We employ an adaptive kernel estimates suggested by Silverman (1986), where the bandwidth $h_{j,t}$ depends on the observation t. This helps to achieve smooth estimates of the tails of the densities by requires a wider bandwidth for the low density region. To ensure different amounts of smoothing in the direction of each variable j, we use variables standardized by their standard deviations.

ditional independence test, we draw $r^*_{t,\tau}$ and $v^*_{1,t}$ independently from the data $\{r_{t,\tau}\}_{t=1}^T$ and $\{v_{1,t}\}_{t=1}^T$ with replacement, respectively. For the conditional independence test, we draw $v^*_{0,t}$ from the data $\{v_{0,t}\}_{t=1}^T$ first. Given $v^*_{0,t}$, we draw $r^*_{t,\tau}$ and $v^*_{1,t}$ independently from the estimated conditional densities $\hat{p}(r_{t,\tau}|v^*_{0,t})$ and $\hat{p}(v_{1,t}|v^*_{0,t})$, respectively.[7] Then, the bootstrap samples, $\{r^*_\tau, v^*_{0,t}, v^*_{1,t}\}_{t=1}^T$, are used to compute the test statistic $\hat{\Gamma}^*$ in the same way $\hat{\Gamma}$ is computed. We draw 10000 bootstrap samples to construct the empirical distribution of $\hat{\Gamma}^*$ under the null hypothesis. When $\hat{\Gamma}$ is greater than the 95th percentile of the empirical distribution of $\hat{\Gamma}^*$, the bootstrap test rejects the null hypothesis at the 5% significance level.

3.2. Estimation of the projected pricing kernel

With the identified state variable, v_t, we can estimate the projected pricing kernel $\tilde{M}_{t,\tau}(r_{t,\tau}, v_t)$. We take a similar approach to that in Aït-Sahalia and Lo (1998). However, different from theirs, we allow the projected pricing kernel to be time-varying. Let $\sigma_{t,\tau}(K)$ be the time-t implied volatility of the option with strike price K and maturity $t+\tau$. Let $H(s_t, K, \tau, \sigma_{t,\tau}(K), r^f_{t,\tau}, \delta_{t,\tau})$ be the Black and Scholes (1973)'s call option pricing formula, where s_t is the underlying asset price, $r^f_{t,\tau}$ is the risk-free rate for maturity τ at t, and $\delta_{t,\tau}$ is the time-t value of the expected dividend stream from t to $t+\tau$. Invoking the well-known results of Breeden and Litzenberger (1978), the conditional risk-neutral density, is given by

$$\tilde{p}(r_{t,\tau}|v_t) = r^f_{t,\tau} s_t \frac{\partial^2 H(s_t, K, \tau, \sigma_{t,\tau}(K), r^f_{t,\tau}, \delta_{t,\tau})}{\partial K^2}|_{K=s_{t+\tau}}. \tag{6}$$

Note that we use the Black-Scholes option pricing formula merely for the transformation from the implied volatility to the option price, and do not rely on the assumptions in the Black-Scholes model to infer the conditional risk-neutral density. For a given t and τ, we estimate the implied volatility function, $\sigma_{t,\tau}(K)$, nonparametrically, using the local linear regression. The local linear regression has advantages over the classical Nadaraya-Watson kernel regression in that the bias at the boundary region arising from the Nadaraya-Watson

[7] We follow the bootstrap approach in Paparoditis and Politis (2000) for sampling from the conditional densities.

kernel regression is absent for the local linear regression. Suppressing the dependence on t and τ, the estimator is the first element of (α, β) that minimizes

$$\sum_{i=1}^{N} [\sigma_i - \alpha - \beta(K_i - K)]^2 \frac{1}{h_K} G\left(\frac{K_i - K}{h_K}\right), \tag{7}$$

where σ_i is the implied volatility at strike price K_i, $G(\cdot)$ is a kernel function, h_K is the bandwidth, and N is the total number of strike prices for maturity $t+\tau$ at t. We use the second order Gaussian kernel and adopt an optimal plug-in bandwidth selection rule that has been shown to exhibit superior asymptotic and practical performance to the cross-validation method.[8] Substituting the fitted implied volatility, $\hat{\sigma}(K)$, to (6), and applying the numerical differentiation, gives the estimator of the conditional risk-neutral density, $\hat{\tilde{p}}(r_{t,\tau}|v_t)$.

Denote $\hat{p}(r_{t,\tau}, v_t)$ as the estimated joint density, based on the Nadaraya-Watson estimator as (5). The conditional actual density is estimated by $\hat{p}(r_{t,\tau}|v_t) = \frac{\hat{p}(r_{t,\tau},v_t)}{\int \hat{p}(r_{t,\tau},v_t)dv_t}$, and the pricing kernel is estimated by $\hat{\tilde{M}}_{t,\tau}(r_{t,\tau}, v_t) = \frac{\hat{\tilde{p}}(r_{t,\tau}|v_t)}{r^f_{t,\tau}\hat{p}(r_{t,\tau}|v_t)}$.[9]

3.3. *Test of the monotonicity of the projected pricing kernel*

For each t and τ, the monotonicity of the projected pricing kernel is examined by testing $D_{t,\tau}(r_{t,\tau}, v_t) \equiv \frac{\partial \tilde{M}_{t,\tau}(r_{t,\tau},v_t)}{\partial r_{t,\tau}} \leq 0$ for all $r_{t,\tau} \in (a_L, a_H)$ against $D_{t,\tau}(r_{t,\tau}, v_t) > 0$ for some $r_{t,\tau} \in (a_L, a_H)$, where (a_L, a_H) covers the region of most density of $r_{t,\tau}$. The test is based on a bootstrap procedure to achieve good finite sample performance. The pointwise bootstrap confidence interval of $\hat{D}_{t,\tau}(r_{t,\tau}, v_t)$, the estimate of $D_{t,\tau}(r_{t,\tau}, v_t)$, is calculated, and the monotonicity of the projected pricing kernel is rejected if the lower bound of the bootstrap confidence interval is above zero for some $r_{t,\tau} \in (a_L, a_H)$.[10] The sampling

[8]The optimal bandwidth minimizes the weighted integrated mean squared error, which is a measure of the expected value of the squared difference between the fitted function and the true function integrated over the range of independent variables. Following the approach of Ruppert et al. (1995), we estimate a pilot for the true implied volatility function using a quadratic function and ordinary least squares estimation.

[9]The approach ensures that the estimated conditional actual density, $\hat{p}(r_{t,\tau}|v_t)$, integrates to one.

[10]The testing procedure is different from the usual hypothesis testing based on bootstrap samples, where the bootstrap confidence intervals are constructed under the null.

variation of $\hat{D}_{t,\tau}(r_{t,\tau}, v_t)$ is from two types of errors, the errors in the estimate $\hat{\tilde{p}}(r_{t,\tau}|v_t)$, through the errors in $\hat{\sigma}_{t,\tau}(K)$, and the errors in the estimate $\hat{p}(r_{t,\tau}|v_t)$. These two types of errors are assumed to be independent when constructing the bootstrap samples. Suppress the dependence on t and τ, and let $\hat{\varepsilon}_i = \sigma_i - \hat{\sigma}_i$ be the residual from the fitted implied volatility for the strike price K_i. The two-point wild bootstrap samples, $\{\sigma_i^*\}_{i=1}^N$, are constructed to account for the sampling variation in $\hat{\sigma}_i$ as

$$\sigma_i^* = \hat{\sigma}_i + \varepsilon_i^*, \tag{8}$$

where $\varepsilon_i^* = \frac{1-\sqrt{5}}{2}\hat{\varepsilon}_i$ with probability $\frac{1+\sqrt{5}}{2\sqrt{5}}$, and $\varepsilon_i^* = \frac{1+\sqrt{5}}{2}\hat{\varepsilon}_i$ with probability $\frac{-1+\sqrt{5}}{2\sqrt{5}}$. The new errors have the following property: $E^*(\varepsilon_i^*) = 0$, $E^*(\varepsilon_i^{*2}) = \hat{\varepsilon}_i^2$ and $E^*(\varepsilon_i^{*3}) = \hat{\varepsilon}_i^3$, where E^* indicates the expected value in the simulation. To account for the sampling variation in $\hat{p}(r_{t,\tau}|v_t)$, the bootstrap samples $\{(r_{t,\tau}^*, v_t^*)\}_{t=1}^T$ are drawn from the data $\{(r_{t,\tau}, v_t)\}_{t=1}^T$ with replacement.[11] The estimate $\hat{D}_{t,\tau}^*(r_{t,\tau}, v_t)$ is calculated from the independent bootstrap samples of $\{\sigma_i^*\}_{i=1}^N$ and $\{(r_{t,\tau}^*, v_t^*)\}_{t=1}^T$ in the same way as $\hat{D}_{t,\tau}(r_{t,\tau}, v_t)$ is calculated from the actual data. If the 5th percentile of the distribution of $\hat{D}_{t,\tau}^*(r_{t,\tau}, v_t)$ is greater than zero for some $r_{t,\tau} \in (a_L, a_H)$, the monotonicity of the projected pricing kernel is rejected at 5%.

3.4. *Economic significance of the nonmonotonicity*

We assess the economic importance of the nonmonotonicity of the projected pricing kernel based on the following measures. The first one is the probability of the nonmonotonicity, defined as

$$\mathrm{PR}_t = \int_0^\infty 1_{\{D_{t,\tau}(r_{t,\tau}, v_t)>0\}} p(r_{t,\tau}|v_t) dr_{t,\tau}. \tag{9}$$

PR_t has a range between zero to one. A high value of PR_t indicates that the nonmonotonicity occurs in the important regions where the density of the index return is high. The second one is the magnitude of the nonmonotonicity, defined as,

$$\mathrm{MG}_t = \int_0^\infty \frac{r_{t,\tau} D_{t,\tau}(r_{t,\tau}, v_t)}{\tilde{M}_{t,\tau}(r_{t,\tau}, v_t)} 1_{\{D_{t,\tau}(r_{t,\tau}, v_t)>0\}} p(r_{t,\tau}|v_t) dr_{t,\tau}. \tag{10}$$

[11] The Kunsch's (1989) block bootstrap method is used to account for the time-series dependence of $(r_{t,\tau}, v_t)$.

MG_t is the density weighted and normalized slope of the increasing section of the projected pricing kernel. MG_t can be compared with the average relative-risk aversion defined as

$$\text{RA}_t = -\int_0^\infty \frac{r_{t,\tau} D_{t,\tau}(r_{t,\tau}, v_t)}{\tilde{M}_{t,\tau}(r_{t,\tau}, v_t)} p(r_{t,\tau}|v_t) dr_{t,\tau}. \tag{11}$$

MG_t measures the degree of risk loving implied by the nonmonotonicity of the projected pricing kernel.

4. Data and Empirical Results

4.1. Data

We use the major equity indexes from various countries to proxy for the aggregate wealth in the empirical analysis, the S&P 500 for the U.S. (SPX), FTSE 100 for the U.K. (UKX), DAX for Germany (DAX), CAC 40 for France (CAC), NIKKEI 225 for Japan (NKY), and HANG SENG for Hong Kong (HSI). The option data on these indexes and zero curve are from OptionMetrics, and data on the index level is from Bloomberg. We use monthly options data with maturity of 30 days to conduct this analysis. Specifically, for each regular monthly maturity, we pick the date when options have 30 days to maturity. Doing so, we avoid introducing errors due to interpolating along the maturity dimension when estimating the risk-neutral density.

First, we select the candidate state variables for estimating the conditional actual densities. Because the same set of state variables jointly determine the conditional risk-neutral and actual densities and the risk premium, we consider a set of state variables embedded in the conditional risk-neutral density, which can be easily calculated from a cross section of option prices. We use the risk-neutral variance, skewness and kurtosis with maturity of 30 days, the same horizon as the index returns and pricing kernel. We use the model-free variance calculated as in Carr and Wu (2009) to estimate the risk-neutral variance and follow the procedure in Bakshi, Kapadia, and Madan (2003) to estimate risk-neutral skewness and kurtosis. The selection is mainly due to the popularity of these measures, especially for the model-free variance and risk-neutral skewness, which are published for major equity indexes by various exchanges. The model-free variance measures the risk-neutral expected 30-day quadratic variation of the underlying asset returns. The well-known volatility index, VIX, is the square root of the model-free variance of the S&P 500 index, constructed by the Chicago Board Options Exchange (CBOE). The volatility indexes for other major indexes are also published by exchanges for various sample periods. When they are not available for certain periods, we calculate these indexes following the procedure of CBOE. The SKEW index constructed by CBOE is the risk-neutral skewness of the S&P 500 index with maturity of 30 days. We calculate the risk-neutral skewness for other indexes, and the risk-neutral kurtosis for all these indexes by ourself.

The summary statistics of monthly returns from t to $t + \tau$, $r_{t,\tau}$, the square root of the risk-neutral variance, risk-neutral skewness and kurtosis, VX_t, SK_t, KT_t, and the sample period for each index are reported in Table 1. For example, the S&P 500 index has an average 30-day return of 0.59% over the sample period from January 1996 to March 2018. The average of the square root of annual risk-neutral variance is about 0.2. The risk-neutral distribution is negative skewed with an average skewness of -2 and leptokurtic with an average kurtosis of 9.6. The risk-neutral moments also have substantial time-series variations. The average returns of other major indexes are positive although the sample periods are different across the indexes. The risk-neutral volatilities of these indexes have an average also around 0.2, and all the indexes have negative risk-neutral skewness and excess kurtosis.

Table 1 here

4.2. Empirical results

Table 2 reports the p-values of testing the state variables in the actual densities. Across all the indexes, the independence between the index return, $r_{t,\tau}$, and risk-neutral volatility, VX_t, are strongly rejected, although for NKY, the test is rejected at a marginal significance level. The independence between $r_{t,\tau}$ and risk-neutral skewness, SK_t, cannot be rejected for SPX, DAX, CAC and NKY, and is rejected at the 5% significance level for UKX and HSI. The independence between $r_{t,\tau}$ and risk-neutral kurtosis, KT_t, cannot be rejected at the conventional significance level for all the indexes. The next two columns show results of testing the independence between $r_{t,\tau}$ and SK_t and between $r_{t,\tau}$ and KT_t conditional on VX_t. The results indicate that conditional VX_t, SK_t or KT_t does provide additional information on the conditional distribution of $r_{t,\tau}$ under the actual probability, except that for HSI, the independence between $r_{t,\tau}$ and SK_t conditional on VX_t is rejected at the 5% significance level. Therefore, in the empirical analysis below, we use VX_t as the only state variable for estimating the actual density of $r_{t,\tau}$.[12]

Table 2 here

The results of testing the monotonicity of the projected pricing kernel are shown in Table 3. We focus on the high density region, i.e., gross return, $r_{t,\tau}$, from 0.9 to 1.1. When the upper bound of the bootstrap confidence bands exceed zero at any point in this region, the monotonicity is rejected. Across the indexes, ranging from 38% to 76% of the monthly observations, the monotonicity is rejected at the 5% significance level. At the 1% significance level, the rejection rates range from 13% for HSI to 40% for UKX. The results suggest that the nonmonotonicity is common among the major equity indexes. The rejection rates for SPX, the mostly examined index in this literature, happens to be right in the middle among the indexes. We further examine in what region of $r_{t,\tau}$, the nonmonotonicity is more likely to occur. We observe some differences across the indexes. For SPX, UKX and HSI, the nonmonotonicity is more likely to occur at the high $r_{t,\tau}$ region, for DAX and CAC, the nonmonotonicity is more likely to occur at the low $r_{t,\tau}$ region, and for NKY, there is no obvious pattern. We further condition the likelihood of the nonmonotonicity on the risk-neutral volatility. To do so, we simply calculate the rejection

[12] Even when some candidate state variables are not rejected by the conditional independence test, these variables can still determine the projected pricing kernel via the conditional risk-neutral densities.

rates when VX_t is below or above the median. Across all the indexes, an interesting pattern shows up. Moving from low VX_t to high VX_t, the rejection rates are reduced in the low $r_{t,\tau}$ region and are increased in the high $r_{t,\tau}$ region.

Table 3 here

We plot the estimated projected pricing kernel on two representative dates, one with high risk-neutral volatility, and the other with low risk-neutral volatility. Figure 1 shows the estimated projected pricing kernel in September 2008 when the risk-neutral volatility is high.[13] It can be seen that the nonmonotonicity of the projected pricing kernel tends to occur at the high return regions across all the indexes. Figure 2 shows the estimated projected pricing kernel in March 2017 when the risk-neutral volatility is low. In contrast to Figure 1, the nonmonotonicity of the projected pricing kernel tends to occur at the low return regions. The figures exemplify the general results reported in Table 2 regarding the different patterns of the nonmonotonicity for different volatility levels.

Figure 1 here

Figure 2 here

The economic significance of the nonmonotonicity of the projected pricing kernel is reported in Table 4. For the probability of nonmonotonicity, PR_t, the average is from 32% to 41% for these indexes. The results suggest that the nonmonotonicity occurs at the non-trivial region of the density, i.e., near the region where $r_{t,\tau} = 1$. For the magnitude, MG_t, its average ranges from 1.55 for HSI to 3.44 for UKX. To understand the magnitude, a measure of relative-risk aversion, RA_t, is also shown. MG_t can be regarded as density

[13] The expiration days for options on various indexes are different. The regular options on SPX, UKX, DAX, and CAC expire on the third Friday in each month. For NKY and HSI, the regular options expire on the second Friday and the second last business day in each month, respectively. Since we select options with 30 days to expiration, the estimated projected pricing kernel for options on different indexes shown in the figures are taken on different days in the month.

weighted average of the slope of the projected pricing kernel only in the region where the slope is positive, whereas RA_t can be regarded as the density weighted average of negative slope for the entire region of $r_{t,\tau}$. For example, the average MG_t is 2.59 and the average RA_t of SPX is 4.09. The results suggest that the magnitude of the nonmonotonicity is large as it plays an important role in determining the overall value of RA_t. For other indexes, especially NKY, MG_t is even more important when compared with RA_t.

Table 4 here

We further examine if the nonmonotonicity of the projected pricing kernel is correlated across indexes. We calculate the correlations of PR_t and MG_t across these indexes over the sample period from January 2006 to March 2018 when the data for all the indexes are available. The results are reported in Table 5. PR_ts are positively correlated among all indexes, except for the pair of NKY and UKX. The magnitudes of the correlations are large even though the timings of the indexes are not matched exactly. Some correlations can be as high as 0.54 for the pair of SPX and HSI. Among all indexes, NKY tends to have lower correlations with other indexes. The correlations of MG_t are also positive and large for most of index pairs. Still, MG_t of NKY has relatively lower correlations with that of other indexes. Overall, the results suggest the nonmonotonicity is systematic across many major equity indexes, and the nonmonotonicity is a robust fact, rather than due to random chances or data errors.

Table 5 here

5. Conclusion

In this paper, we propose new approaches to estimating the projected pricing kernel on equity market indexes and testing the nonmonotonicity of the projected pricing kernel. Our approach allows the projected pricing kernel to be state-dependence, and the state variables governing the dynamics of the projected pricing kernel are determined by the (conditional) independence test supplemented by a bootstrap procedure. The approach is nonparametric, without assuming the functional of the pricing kernel. Our estimation approach avoids the restrictive parametric assumptions and the ad hoc choice of the state variables in the literature. We also construct metrics to measure the economic significance of the nonmonotonicity if the nonmonotonicity is identified.

The approach is applied to many major equity indexes around the world. We find that the nonmonotonicity happens very frequently, in about a half of the monthly observations on average. The nonmonotonicity can occur in low, medium or high regions in the return distribution, and the likelihood of nonmonotonicity in the high (low) return region increases (decreases) when the conditional volatility increases. The nonmonotonicity is economically significant since nonmonotonicity appears at the high density region of the return distribution in general and the slope of the increasing section of the projected pricing kernel is steep. The measures of economic significance of the nonmonotonicity tend to be positively correlated across the indexes in the time series. Overall, our results suggest that the nonmonotonicity is economically significant and systematic, and the patterns of the nonmonotonicity across many major indexes are similar. Our results also provide a foundation for the understanding the economic reasons behind the nonmonotonicity in future studies.

References

Aït-Sahalia, Y. and A. Lo, 2000, Nonparametric risk management and implied risk aversion, Journal of Econometrics, 94, 9-51.

Bakshi G., D. Madan, and G. Panayotov, 2010, Returns of claims on the upside and the viability of U-shaped pricing kernels, Journal of Financial Economics, 97, 130-154.

Barone-Adesi, G., R. F. Engle, and L. Mancini, 2008, A GARCH option pricing model with filtered historical simulation, Review of Financial Studies, 21, 1223-1258.

Beare, B. K. and L. D. W. Schmidt, 2016, An empirical test of pricing kernel monotonicity, Journal of Applied Econometrics, 31, 338-356.

Bliss, R. R. and N. Panigirtzoglou, 2004, Option implied risk aversion estimate, Journal of Finance, 59, 407-446.

Breeden, D. T. and R. H. Litzenberger, 1978, Prices of state-contingent claims implicit in options prices, Journal of Business, 51, 621-651.

Carr, P., and L. Wu, 2009, Variance risk premiums, Review of Financial Studies, 22, 1311-1341.

Chaudhuri, R. and M. Schroder, 2015, Monotonicity of the stochastic discount factor and expected option returns, Review of Financial Studies, 28, 1462-1505.

Coval, Joshua D. and Tyler Shumway, 2001, Expected option returns, Journal of Finance, 56, 983-1009.

Cuesdeanu. H. and J. C. Jackwerth, 2018, The pricing kernel puzzle: survey and outlook, Annals of Finance, 14, 289-329.

Fernandes, M. and B. Néri, 2010, Nonparametric entropy-based tests of independence between stochastic processes, Econometric Reviews, 29, 276-306.

Grith, M., W. K. Härdle, and J. Park, 2013, Shape invariant modeling pricing kernels and risk aversion, Journal of Financial Econometrics, 11, 370-399.

Jackwerth, J. C., 2000, Recovering risk aversion from option prices and realized returns, Review of Financial Studies, 13, 433-451.

Kunsch, H. R., 1989, The jack knife and the bootstrap for general stationary observations. Annals of Statistics, 17, 1217-1241.

Linn, M., S. Shive, and T. Shumway, 2018, Pricing kernel monotonicity and conditional information, Review of Financial Studies, 31, 493-531.

Liu, X., M. B. Shackleton, S. J. Taylor, and X. Xu, 2009, Empirical pricing kernels obtained from the UK index options market, Applied Economic Letters, 16, 989-993.

Paparoditis, E. and D. N. Politis, 2000, The local bootstrap for kernel estimators under general dependence conditions. Annals of the Institute of Statistical Mathematics, 52, 139-159.

Perignon, C., and C. Villa, 2002, Extracting information from options markets: smiles, state-price densities and risk aversion, European Financial Management, 8, 495-513.

Rosenberg, J. V. and R. F. Engle, 2002, Empirical pricing kernels, Journal of Financial Economics, 64, 341-372.

Ruppert, D., S. Sheather, and M. Wand, 1995, An effective bandwidth selector for local least squares regression, Journal of American Statistical Association, 90, 1257-1270.

Silverman, B. W., 1986, Density Estimation for Statistics and Data Analysis, Chapman and Hall, New York.

Song, Z. and D. Xiu, 2016, A tale of two option markets: Pricing kernels and volatility risk, Journal of Econometrics, 190, 176-196.

Su, L. and H. White, 2008, A nonparametric Hellinger metric test for conditional independence, Econometric Theory, 24, 829-864.

Table 1
Summary statistics
This table reports the mean, standard deviation (std), the 5th, 25th, 50th, 75th, and 95th percentiles of monthly observations of 30-day return from t to $t+\tau$, $r_{t,\tau}-1$, and 30-day risk-neutral volatility, VX_t, skewness, SK_t, and kurtosis, KT_t, observed at t. Panels A-F are for the S&P 500 index for the U.S. (SPX), the FTSE 100 index for the U.K. (UKX), the DAX index for Germany (DAX), the CAC 40 index for France (CAC), the NIKKEI 225 index for Japan (NKY), and the HANG SENG index for Hong Kong (HSI), respectively. The sample period for each panel is also reported.

A. SPX: 199601-201803							
	mean	std	p5	p25	p50	p75	p95
$r_{t,\tau}-1$	0.0059	0.0465	-0.0720	-0.0173	0.0108	0.0362	0.0710
VX_t	0.2013	0.0857	0.1108	0.1434	0.1857	0.2345	0.3555
SK_t	-2.0449	0.7838	-3.6094	-2.4990	-1.9770	-1.4400	-1.0312
KT_t	9.5930	4.9037	4.9513	6.5581	8.3966	10.8742	19.0096
B. UKX: 200201-201803							
	mean	std	p5	p25	p50	p75	p95
$r_{t,\tau}-1$	0.0027	0.0452	-0.0786	-0.0221	0.0095	0.0313	0.0699
VX_t	0.1912	0.0909	0.1085	0.1321	0.1608	0.2169	0.3824
SK_t	-1.6856	0.6449	-3.0113	-1.9275	-1.5393	-1.2807	-0.9539
KT_t	10.4412	6.9943	4.9835	6.6016	8.5502	11.3747	22.3025
C. DAX: 200201-201803							
	mean	std	p5	p25	p50	p75	p95
$r_{t,\tau}-1$	0.0052	0.0608	-0.0953	-0.0324	0.0138	0.0471	0.0932
VX_t	0.2335	0.1025	0.1351	0.1659	0.2042	0.2624	0.4649
SK_t	-1.5268	0.4951	-2.5199	-1.7890	-1.4422	-1.1824	-0.8826
KT_t	9.7812	5.1937	4.8225	6.5574	8.0395	11.9050	18.7805
D. CAC: 200304-201803							
	mean	std	p5	p25	p50	p75	p95
$r_{t,\tau}-1$	0.0039	0.0539	-0.0898	-0.0284	0.0127	0.0417	0.0800
VX_t	0.2147	0.0819	0.1291	0.1574	0.1929	0.2439	0.3564
SK_t	-1.4230	0.4318	-2.1741	-1.6668	-1.3528	-1.1324	-0.8306
KT_t	8.1178	3.5950	4.2774	5.8445	7.4083	9.5172	15.2976

Table 1
Summary statistics (cont'd)

E. NKY: 200405-201803							
	mean	std	p5	p25	p50	p75	p95
$r_{t,\tau} - 1$	0.0035	0.0675	-0.1029	-0.0328	0.0031	0.0428	0.0998
VX_t	0.2426	0.0929	0.1431	0.1812	0.2266	0.2779	0.4046
SK_t	-1.2158	0.7127	-2.3995	-1.5012	-1.1122	-0.7451	-0.3123
KT_t	8.7387	6.1881	3.8004	5.4234	7.1017	9.4017	17.8674
F. HSI: 200601-201803							
	mean	std	p5	p25	p50	p75	p95
$r_{t,\tau} - 1$	0.0074	0.0632	-0.1095	-0.0266	0.0124	0.0443	0.1104
VX_t	0.2370	0.1160	0.1330	0.1652	0.2009	0.2785	0.4744
SK_t	-0.8340	0.3857	-1.3834	-1.0572	-0.7952	-0.5772	-0.3212
KT_t	4.9584	1.4442	3.5574	3.9745	4.5177	5.5627	7.5900

Table 2
Testing the conditioning variables
This table reports p-values of testing the independence between 30-day gross return from t to $t+\tau$, $r_{t,\tau}$, and 30-day risk-neutral volatility at t, VX_t, between $r_{t,\tau}$ and 30-day risk-neutral skewness at t, SK_t, and between $r_{t,\tau}$ and 30-day risk-neutral kurtosis, KT_t. The last two columns show the p-values of testing the independence between $r_{t,\tau}$ and SK_t and between $r_{t,\tau}$ and KT_t, respectively, conditional on VX_t. SPX is for the S&P 500 index, UKX is for the FTSE 100 index, DAX is for the DAX index, CAC is for the CAC 40 index, NKY is for the NIKKEI 225 index, and HSI is for the HANG SENG index.

	$r_{t,\tau}, \mathrm{VX}_t$	$r_{t,\tau}, \mathrm{SK}_t$	$r_{t,\tau}, \mathrm{KT}_t$	$r_{t,\tau}, \mathrm{SK}_t \vert \mathrm{VX}_t$	$r_{t,\tau}, \mathrm{KT}_t \vert \mathrm{VX}_t$
SPX	0.000	0.492	0.542	0.757	0.790
UKX	0.000	0.021	0.113	0.119	0.269
DAX	0.000	0.486	0.551	0.623	0.757
CAC	0.000	0.106	0.168	0.279	0.724
NKY	0.015	0.173	0.341	0.350	0.397
HSI	0.000	0.009	0.053	0.029	0.063

Table 3
Rejection rates of the monotonicity tests
This table reports rejection rates of the monthly monotonicity tests at the 5% and 1% significance levels. The row labeled by Overall indicates the overall rejection rates for the region where $r_{t,\tau} \in [0.9, 1.1)$. The rejection rates for $r_{t,\tau} \in [0.9, 0.97)$, $r_{t,\tau} \in [0.97, 1.03)$, and $r_{t,\tau} \in [1.03, 1.1)$ are reported separately in the row labeled by All VX_t. For each of the three regions in $r_{t,\tau}$, the rejection rates conditional on the risk-neutral volatility below or above the median, are labeled by Low VX_t and High VX_t, respectively. Panels A-F are for the S&P 500 index (SPX), the FTSE 100 index (UKX), the DAX index (DAX), the CAC 40 index (CAC), the NIKKEI 225 index (NKY), and the HANG SENG index (HSI), respectively.

A. SPX						
		5%			1%	
Overall		0.4549			0.2782	
$r_{t,\tau}$	[0.9,0.97)	[0.97,1.03)	[1.03,1.1)	[0.9,0.97)	[0.97,1.03)	[1.03,1.1)
All VX_t	0.0602	0.1955	0.3045	0.0226	0.0489	0.2030
Low VX_t	0.1203	0.0752	0.0526	0.0451	0.0376	0.0301
High VX_t	0.0000	0.3158	0.5564	0.0000	0.0602	0.3759
B. UKX						
		5%			1%	
Overall		0.6031			0.4021	
$r_{t,\tau}$	[0.9,0.97)	[0.97,1.03)	[1.03,1.1)	[0.9,0.97)	[0.97,1.03)	[1.03,1.1)
All VX_t	0.0876	0.1134	0.4897	0.0309	0.0412	0.3402
Low VX_t	0.1753	0.2062	0.3093	0.0619	0.0825	0.1546
High VX_t	0.0000	0.0206	0.6701	0.0000	0.0000	0.5258
C. DAX						
		5%			1%	
Overall		0.7577			0.3763	
$r_{t,\tau}$	[0.9,0.97)	[0.97,1.03)	[1.03,1.1)	[0.9,0.97)	[0.97,1.03)	[1.03,1.1)
All VX_t	0.4742	0.2113	0.1186	0.3196	0.0412	0.0103
Low VX_t	0.9175	0.0825	0.0000	0.6392	0.0103	0.0000
High VX_t	0.0309	0.3402	0.2371	0.0000	0.0722	0.0206
D. CAC						
		5%			1%	
Overall		0.3807			0.1761	
$r_{t,\tau}$	[0.9,0.97)	[0.97,1.03)	[1.03,1.1)	[0.9,0.97)	[0.97,1.03)	[1.03,1.1)
All VX_t	0.2045	0.0114	0.1761	0.1023	0.0000	0.0682
Low VX_t	0.3864	0.0227	0.1023	0.2045	0.0000	0.0341
High VX_t	0.0227	0.0000	0.2500	0.0000	0.0000	0.1023

Table 3
Rejection rates of the monotonicity tests (cont'd)

E. NKY						
	5%			1%		
Overall		0.5333			0.2727	
$r_{t,\tau}$	[0.9,0.97)	[0.97,1.03)	[1.03,1.1)	[0.9,0.97)	[0.97,1.03)	[1.03,1.1)
All VX_t	0.2667	0.2848	0.2242	0.1212	0.1576	0.1273
Low VX_t	0.5181	0.0602	0.0000	0.2410	0.0482	0.0000
High VX_t	0.0122	0.5122	0.4512	0.0000	0.2683	0.2561
F. HSI						
	5%			1%		
Overall		0.3973			0.1301	
$r_{t,\tau}$	[0.9,0.97)	[0.97,1.03)	[1.03,1.1)	[0.9,0.97)	[0.97,1.03)	[1.03,1.1)
All VX_t	0.0822	0.1164	0.3082	0.0411	0.0068	0.0890
Low VX_t	0.1644	0.0274	0.1644	0.0822	0.0000	0.0685
High VX_t	0.0000	0.2055	0.4521	0.0000	0.0137	0.1096

Table 4
Economic signficance of the nonmonotonicity of the projected pricing kernel
This table reports the mean and standard deviation (std) of the probability of the nonmonotonicity, PR_t, defined as (9), the magnitude of the nonmonotonicity, MG_t, defined as (10), and the relative-risk aversion, defined as (11). SPX is for the S&P 500 index, UKX is for the FTSE 100 index, DAX is for the DAX index, CAC is for the CAC 40 index, NKY is for the NIKKEI 225 index, and HSI is for the HANG SENG index.

	SPX			UKX		
	PR_t	MG_t	RA_t	PR_t	MG_t	RA_t
mean	0.3745	2.5933	4.0904	0.3859	3.4354	3.1128
std	0.1569	1.6726	4.6807	0.1265	2.1413	4.4832
	DAX			CAC		
	PR_t	MG_t	RA_t	PR_t	MG_t	RA_t
mean	0.3605	2.6575	3.4600	0.4094	2.0587	2.3557
std	0.1369	0.8281	3.3138	0.1436	1.1295	2.8659
	NKY			HSI		
	PR_t	MG_t	RA_t	PR_t	MG_t	RA_t
mean	0.3818	2.4485	1.9355	0.3159	1.5497	4.1722
std	0.1273	1.3595	2.7675	0.1741	0.9064	4.1340

Table 5
Correlations of PR_t and MG_t among indexes
This table reports time-series correlations of the probability of the nonmonotonicity, PR_t, defined as (9), and the magnitude of the nonmonotonicity, MG_t, defined as (10) across the indexes. SPX is for the S&P 500 index, UKX is for the FTSE 100 index, DAX is for the DAX index, CAC is for the CAC 40 index, NKY is for the NIKKEI 225 index, and HSI is for the HANG SENG index.

A. PR_t					
	SPX	UKX	DAX	CAC	NKY
UKX	0.5290				
DAX	0.4685	0.2863			
CAC	0.1424	0.2339	0.2520		
NKY	0.1383	-0.0921	0.3163	0.0133	
HSI	0.5438	0.3452	0.5241	0.2109	0.0880
B. MG_t					
	SPX	UKX	DAX	CAC	NKY
UKX	0.3770				
DAX	0.3086	0.3666			
CAC	0.3736	0.4439	0.4798		
NKY	0.1966	0.0424	0.1293	-0.0561	
HSI	0.1737	0.1536	0.0069	0.0625	0.1601

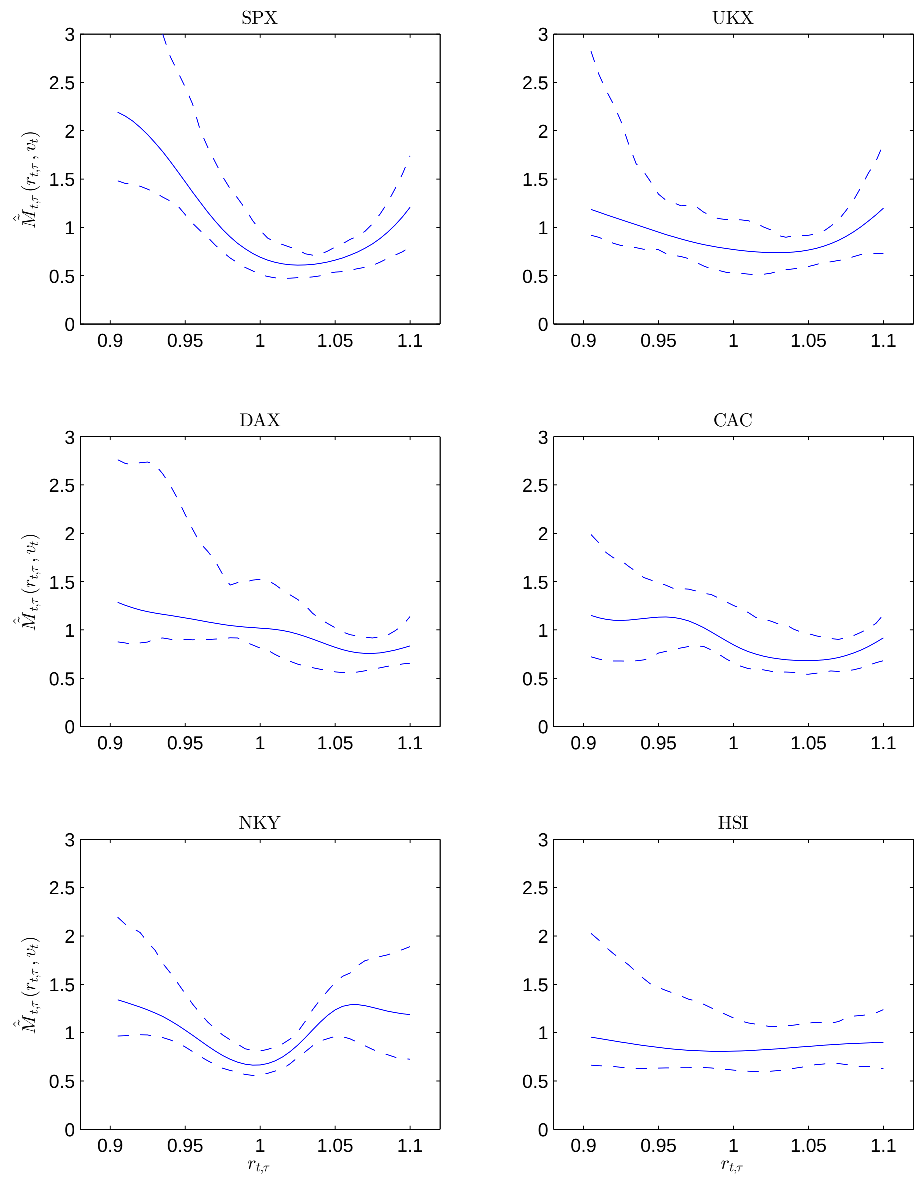

Figure 1. Estimated projected pricing kernel in September 2008

This figure shows estimated projected pricing kernel on a day in September 2008 for various indexes. The solid line is the mean estimate, and the dash lines are the 90% confidence band. SPX is for the S&P 500 index, UKX is for the FTSE 100 index, DAX is for the DAX index, CAC is for the CAC 40 index, NKY is for the NIKKEI 225 index, and HSI is for the HANG SENG index.

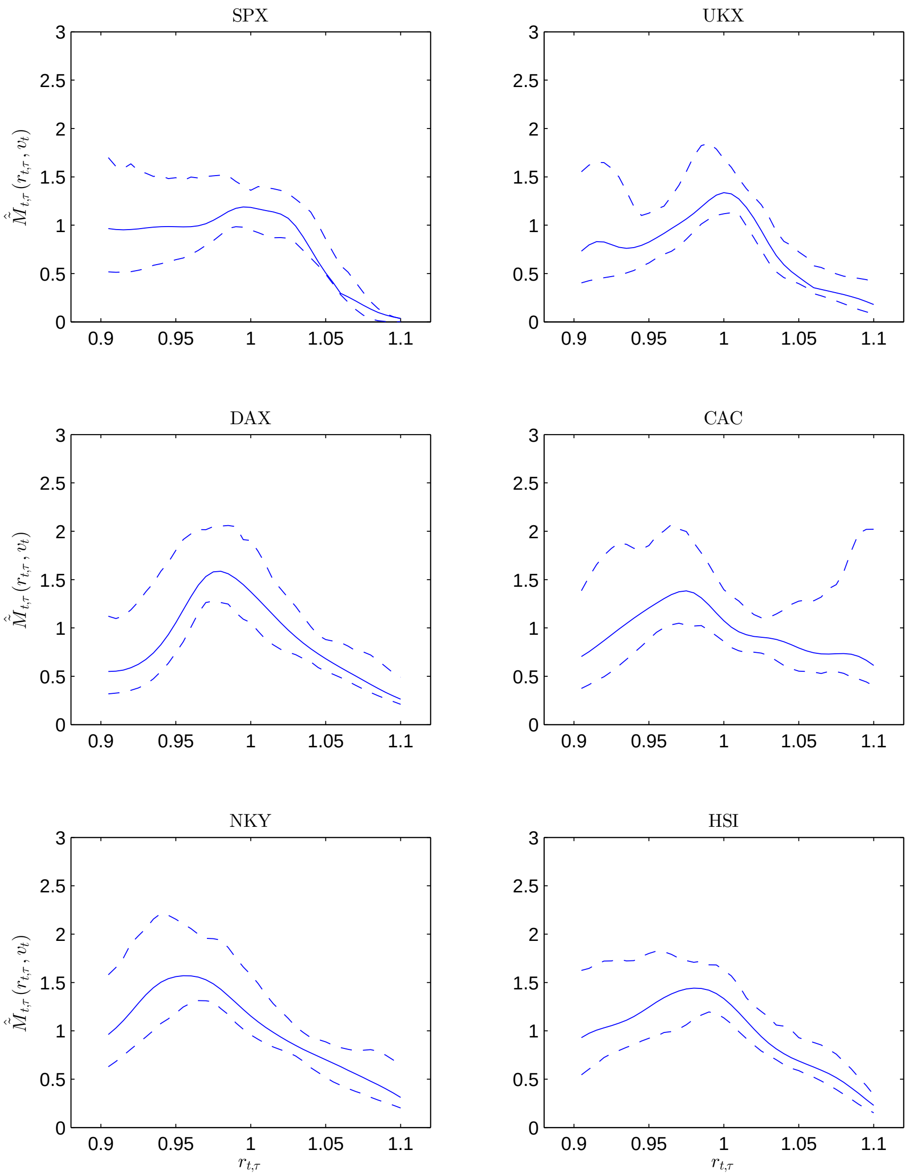

Figure 2. Estimated projected pricing kernel in March 2017

This figure shows estimated projected pricing kernel on a day in March 2017 for various indexes. The solid line is the mean estimate, and the dash lines are the 90% confidence band. SPX is for the S&P 500 index, UKX is for the FTSE 100 index, DAX is for the DAX index, CAC is for the CAC 40 index, NKY is for the NIKKEI 225 index, and HSI is for the HANG SENG index.